JPET Fast Forward. Published on February 20, 2003 as DOI:10.1124/jpet.102.046201

JPET/2002/46201

STREPTOZOTOCIN-INDUCED DIABETES INCREASES DISULFIDE BOND FORMATION ON CARDIAC RYANODINE RECEPTOR (RyR2)

Keshore R. Bidasee[1], Karuna Nallani[2], Henry R. Besch, Jr[2,3,4] and U. Deniz Dincer[5]

[1]Department of Pharmacology University of Nebraska Medical Center, Omaha, Nebraska, 68198-6260 (K.R.B), [2]Departments of Pharmacology and Toxicology, [3]Medicine and [4]Center for Vascular Biology, Indiana University School of Medicine, Indianapolis, Indiana, USA and [5]Department of Pharmacology, Faculty of Pharmacy, University of Ankara, Tandogan, Ankara, Turkey

(a) Running title: STZ-diabetes increases disulfide bonds on RyR2

(b) Address correspondence to:

Keshore R. Bidasee, Ph.D. Department of Pharmacology, University of Nebraska Medical Center, 986260 Nebraska Medical Center Omaha, NE 68198-6260

telephone: (402) 559-9018, fax: (402) 559-7495, email: kbidasee@unmc.edu

(c) Number of text pages: 43

Number of tables: 1

Number of figures: 11

Number of references: 40

Number of words in abstract: 247

Number of words in introduction: 580

Number of words in discussion: 1319

(d) abbreviations: type 2 ryanodine receptor, RyR2; streptozotocin, STZ; sulfhydryl groups, SH.

(e) Recommended section assignment: (1) Cardiovascular

Abstract

In a previous study we showed that after 6-weeks of streptozotocin-induced diabetes (6D), expression of type 2 ryanodine receptor calcium-release channels (RyR2) did not change significantly in rat hearts. However, the ability of this protein to bind [^{3}H]ryanodine was compromised (Bidasee et al., 2001). Loss in activity therefore resulted from diabetes-induced increases in post-translational modifications on RyR2. In the present study the effects of diabetes on one type of modification, namely changes in oxidative state of reactive sulfhydryls was investigated. RyR2 protein from 6D bound 42.3 ± 7.6 less [^{3}H]ryanodine than RyR2 from controls (6C). The loss in binding was minimized with two weeks of insulin-treatment initiated after 4-weeks of diabetes (77.8 ± 5.5 % of 6C). Pre-treating RyR2 from 6D with 2mM dithiothreitol *in vitro* increases [^{3}H]ryanodine binding by 60.8 ± 5.3%. Dithiothreitol-pretreatment of RyR2 from 6C increased [^{3}H]ryanodine binding by 16.8 ± 4.3%. The reagent pyrocoll interacts with distinct classes of free sulfhydryl groups on 6C RyR2 to induce two major effects. At concentrations ≤ 10μM, it deactivates RyR2 (decreases [^{3}H]ryanodine binding), while at higher concentrations it activates them (increases [^{3}H]ryanodine binding). This reagent was unable to activate RyR2 from 6D. While RyR2 from insulin-treated animals was deactivated by low concentrations of pyrocoll, it was only partially activated at higher concentrations. These data suggest that the dysfunction of RyR2 induced by diabetes may be due in part to formation of disulfide

bonds between adjacent sulfhydryl groups and that these changes were attenuated with insulin treatment.

Individuals with diabetes mellitus (both type 1 and type 2) usually develop cardiovascular complications (Rubler et al., 1972; Hamby et al., 1974; Asmal et al., 1980). While pathologies such as nephropathy, arteriosclerosis and microangiopathy may contribute to the syndrome, a significant body of evidence suggests that these complications could arise primarily from a dysfunction of the heart. This "diabetic cardiomyopathy" (DC) as it is referred to, starts off with a slowing in relaxation kinetics (left ventricular diastolic dysfunction). In most individuals, this early dysfunction usually goes unnoticed since it is asymptomatic and does not normally interfere with daily tasks (Koistinen, 1990). However, as the syndrome progresses systolic function also becomes compromised and the latter increases the incidence of morbidity and mortality in this patient group (Fein, 1990; Janka, 1996).

Cardiac contractility depends critically on the efficient release of calcium ions from the sarcoplasmic reticulum (SR). Yu and McNeill (1991) showed that after 6-weeks of untreated diabetes (induced with 65mg/kg streptozotocin-STZ), post-rest potentiation is compromised in rat hearts. These workers later suggested that diabetes-induced decreases in systolic function might be due in part to decreased expression of type 2 ryanodine receptor calcium-release channels (RyR2) (Yu et al., 1994). Data to support this notion was recently provided by other labs (Teshima et al., 2000, Netticadan et al., 2001; Zhong et al., 2001).

Using 50mg/kg STZ (middle of the dose-response curve, see Rodrigues et al., 1998), we also showed that expression of RyR2 decreases with diabetes, but the decrease occurred after 8-weeks of diabetes (Bidasee et al., 2002). Interestingly, although expression did not change significantly after 6-weeks of diabetes, the ability of

RyR2 to bind the specific ligand [^{3}H]ryanodine was significantly lowered (Bidasee et al., 2001, 2002). These data suggest that prior to a decrease in expression, the activity of RyR2 become compromised. While the mechanism(s) underlying the dysfunction of RyR2 remains undefined, it is likely to be due to diabetes-induced increases in post-translational modifications.

Two major categories of post-translational modifications are envisioned. First, elevation in circulating levels of aldose and ketose sugars triggered by diabetes is likely to increase Schiff base formation on lysine, arginine, cysteine and histidine residues (non-enzymatic glycation reactions) on numerous proteins, including those on RyR2 (Wolf et al., 1991). Over time (≈ 24 - 48hrs), these Schiff bases can undergo internal rearrange to form more stable Amadori products (Baynes et al., 1989). On long-lived proteins, Amadori products can further rearrange to form advanced-glycation end products (Brownlee et al., 1988; Bucala and Cerami, 1992). Secondly, it is well known that metabolic shifts brought about by diabetes increase production of reactive oxygen (e.g., superoxide anions- $O^{\cdot}$, hydroxy radicals- $OH^{\cdot}$, lipid peroxides- $ROO^{\cdot}$, singlet oxygen-$^{1}O_2$, hydrogen peroxide- H_2O_2) and nitrogen species (e.g., nitrosonium cation – NO^{+}, nitroxyl anion- NO^{-}, peroxynitrite- $ONOO^{-}$) (Wolff et al., 1991; Dhalla et al., 2000; Evans et al., 2002). These species (free radicals as well as non-radicals) are also capable of reacting with several amino acid residues on proteins. Like glycation, modification of amino acid residues by reactive oxygen and nitrogen species can alter the tertiary structure of RyR2 and these changes in turn could alter the sensitivity of RyR2 to endogenous ligands leading to a loss in activity.

In the present study the effect of diabetes on one type of post-translational modification, namely alteration in oxidative state of sulfhydryl groups (SH) on RyR2 was investigated. We also investigated whether changes to RyR2 induced by diabetes could be minimized with 2-weeks of insulin-treatment, initiated after 4-weeks of diabetes.

Methods

Chemicals and drugs. Streptozotocin (STZ) and dithiothreitol used in this study were obtained from Sigma-Aldrich (St Louis, MO). Mouse monoclonal anti-RyR2 antibodies were obtained from Affinity Bioreagents Inc., (Golden, CO). Actin antibodies (C-11) were purchased from Santa Cruz Biotechnology (Santa Cruz, CA). Ryanodine was isolated from chipped *Ryania* wood supplied by Integrated Biotechnology Corporation (Carmel, IN) and purified by chromatography to ≥ 98%. [^{3}H]ryanodine (specific activity 56 Ci/mmol) was purchased from NEN Life Sciences Products (Boston, MA). Brevital® (methohexital sodium) and NPH Ilentin II (intermediate-acting insulin) were obtained from Eli Lilly & Co. (Indianapolis, IN). Oligo-primers for RyR2 and β-actin were obtained from Integrated DNA Technologies (Coralville, IA). All other reagents and solvents used were of analytical grade.

Induction and verification of experimental STZ-induced diabetes. All animal procedures were done in accordance with institutional guidelines established by the Institutional Animal Care and Use Committees. Male Sprague-Dawley rats weighing between 180-190g were purchased from Harlan Laboratories (Indianapolis, IN). After anesthesia (Brevital®, 25mg/kg i.p.), animals were injected with either a single dose of STZ (50mg/kg) in 0.1M citrate buffer, pH 4.5 or citrate buffer via their tail veins. Three days later, blood glucose levels were measured using a Glucometer II and Glucostix (Peridochrom Glucose GOD-PAP Assay Kit, Roche Molecular Biochemicals, Indianapolis, IN) to ensure induction of diabetes. Blood sugar and body weights were monitored on weekly basis thereafter. Throughout the study, animals were housed in

pairs (similar weights to minimize dominance) at 22^0C with fixed 12hr light/12hr dark cycles with free access to food and water.

Insulin-treatment protocols. Four weeks after the initial STZ injections, diabetic animals were randomly divided into two groups. One group of these animals was placed on an insulin regimen (NPH Ilentin II - intermediate acting) for two weeks. Insulin doses were individually adjusted so as to maintain euglycemic states and varied between 10 and 15 U/kg (s. c.), given once per day between 9:00 and 11:00 A.M. The other group of diabetic animals continued as non-treated diabetics for two additional weeks.

Sample collection. At the end of the *in vivo* protocol, animals were anesthetized using a single dose of Brevital® (75mg/kg) given i.p. Abdominal cavities were opened and blood samples were collected via the left renal arteries for analysis of plasma glucose, insulin and HbA_{1c} content. Hearts from each group were removed, quick-frozen and then divided into two sub-groups. The smaller sub-group (3-hearts) was marked for determination of mRNA encoding RyR2, while the larger sub-group (9 hearts) was used for determination RyR2 protein content as well as for functional studies.

Determining steady-state levels of RyR2 in hearts from 6-week STZ-diabetic, 4-week STZ-diabetic/2-week insulin-treated and 6-week age matched control rats:

(1) Quantitation of mRNA encoding RyR2:

Total RNA was extracted simultaneously from control, STZ-diabetic and insulin-treated rat hearts using Quick Prep® total RNA extraction kit (Amersham Pharmacia Biotech (Piscataway, NJ). At the end of the procedure, samples were re-suspended in 1ml of diethylpyrocarbonate-treated water (pH 7.5) and RNA concentrations were determined as described previously (Bidasee et al., 2001, 2002). Equivalent amounts of total RNA from each of control, STZ-diabetic and insulin-treated animals were then used to synthesis 1st strand cDNAs. Thereafter, polymerase chain reactions were used to simultaneously amplify cDNAs encoding RyR2 and β-actin. Primers used were as follows: RyR2: sense (GTGTTTGGATCCTCTGCAGTTCAT) and anti-sense (AGAGGCACAAAGAGGAATTCGG) and β-actin: sense (CGTAAAGACCTCTATGC CA) and anti-sense (AGCCATGCCAAATGTCTCAT).

(2) Quantitation of RyR2 protein:

Membrane vesicles were prepared simultaneously from control, STZ-diabetic and insulin-treated rat hearts (3 hearts per preparation X 3 preparations) as described previously (Bidasee et al., 2001, 2002). The protein concentration of each vesicle preparation was then determined. Relative levels of RyR2 protein in hearts from control, STZ-diabetic and insulin-treated rats were then determined as follows. First, one hundred micrograms (100µg) of membrane vesicles from each preparation and varying amount of purified RyR2 (50 to 400ng) were denatured and electrophoresed for 3.5hrs (150V) on 4-20% linear gradient gels. At the end of this time, gels were stained with Coomassie® blue dye, destained overnight and then dried between cellophane sheets. Gels were then scanned and the intensity of the RyR2 band in each membrane

vesicle preparation as well as RyR2 calibration curve were determined using NIH Image (Version 1.62, Bethesda MD). The amount of RyR2 protein in each preparation was then determined by interpolation on the RyR2 calibration curve.

Western blot analyses were carried out to confirm that relative levels of RyR2 protein in each membrane preparation using β-actin as the internal standard to correct for sample load.

Ability of RyR2 from 6-week STZ-diabetic, 4-week STZ-diabetic/2-week insulin-treated and 6-week age matched control rats to bind [^{3}H]ryanodine. The functional integrity of RyR2 from control, STZ-diabetic and insulin-treated rat hearts was assessed from their ability to bind the specific ligand [^{3}H]ryanodine. For this, 100μg/ml total membrane protein from 6-week control, 6-week STZ-diabetic, and 4-week STZ-induced diabetic/2-week insulin treated animals were incubated in binding buffer (500mM KCl, 20mM Tris.HCl and 300μM $CaCl_2$, 0.1mM EGTA, 6.7nM [^{3}H]ryanodine, pH 7.5) for 2 hr at 37^{0}C. After incubation, membranes were filtered, washed and the amount of [^{3}H]ryanodine bound to RyR2 was determined by liquid scintillation counting. Non-specific binding was simultaneously determined by also incubating vesicles with 1μM unlabeled ryanodine. [^{3}H]ryanodine bound to each preparation was then normalized per μg RyR2 protein in that preparation.

The affinities of ryanodine for RyR2 from control, STZ-diabetic and insulin-treated rats were also determine using binding assays. These experiments were conducted as described above except that increasing concentrations of unlabeled ryanodine (0 to

300nM) were added to the samples. IC_{50} values were determined using the binding analysis software of GraphPad Prism 3.0a (PrismPad Software Inc., San Diego, CA) while K_d values were calculated as described previously (Bidasee et al., 2001).

Effect of diabetes on oxidative state of SH groups on RyR2: Studies have shown reagents that interact with or conditions that promote oxidation of SH groups can alter the activity of RyR2 (Trimm et al., 1986; Liu et al., 1994; Aghdasi et al., 1997; Anzai et al., 1998; Sun et al., 2001). These reagents and conditions do so by increasing disulfide bond formation. If the shift in metabolism brought about by diabetes increases oxidative stress, then by extension, SH groups on RyR2 (as well as other proteins) are likely to become oxidized. If the latter occurs, then cysteines residues that are in close proximity to each other will form disulfide bonds (S-S) and this can cause alteration in the tertiary structure of RyR2, leading to a decrease in its ability to bind the specific ligand [^{3}H]ryanodine. Reducing these disulfide bonds should be able to restore [^{3}H]ryanodine binding to RyR2. To test this hypothesis, 100µg/ml vesicle protein from 6-week STZ-diabetic and age-matched control rat hearts were incubated in binding buffer (500mM KCl, 20mM Tris.HCl and 300µM $CaCl_2$, 0.1mM EGTA, 6.7nM [^{3}H]ryanodine, pH 7.4) for 2 hr at 37^{0}C with a reducing concentration of dithiothreitol (2mM). Non-specific binding was simultaneously determined by incubating vesicles with 1µM unlabeled ryanodine. After incubation, vesicles were filtered, washed and the amount of [^{3}H]ryanodine bound to RyR2 was determined by liquid scintillation counting.

[^{3}H]ryanodine bound was then normalized per µg of RyR2 protein. As a control, binding studies were also carried out using an oxidizing concentration of dithiothreitol (500µM). If our hypothesis holds, this lower concentration of dithiothreitol (500µM) should decrease binding of [^{3}H]ryanodine to RyR2 from control animals.

Synthesis of 5H,10H-dipyrrolo[1,2-a:1',2'-d]pyrazine-5,10-dione (pyrocoll).

Compounds with conjugated carbonyl functionality (e.g., 2, 5-cyclohexadiene-1,4-dione, benzoquinone, etc.) are known to react with SH groups (Feng et al.,1999; Weis et al., 1992). In the case of RyR2, which has ≈ 84 free SH residues (≥ 360 cysteine residues total), oxidation of these groups will alter the activity of the channel (either increasing or decreasing activity). We and others have also shown that the pyrrole moiety is an essential determinant for ryanodine to bind to RyR (Welch et al., 1996; Bidasee and Besch, 1998). With these two pieces of information, we rationalized that a sulfhydryl reagent containing a pyrrole moiety might be useful to probe the oxidative state of cysteine residues in close proximity to (or within) the vicinity of the ryanodine binding site(s) on RyR2. Searching the literature, we found a signature molecule that satisfied these criteria, namely the pyrrole-containing quinone, 5H,10H-dipyrrolo[1,2-a:1',2'-d]pyrazine-5,10-dione (also known as pyrocoll). However, a commercial source for this compound was not readily available, nor was there any literature on its sulfhydryl activity. As such, we needed to synthesize pyrocoll as well as evaluate its sulfhydryl activity.

A scheme was devised to synthesize pyrocoll from pyrrole-2-carboxylic acid (see Figure 1). For this, pyrrole-2-carboxylic acid (1g, 9.1mmol) and dried 1,3-

dicylohexylcarbodiimide (2 grams, 9.7mmol) and were added to 25ml of carbon tetrachloride and allowed to react for 2hr at room temperature employing continuous stirring. At the end of this time, 1ml of distilled water was added to the reaction and the precipitate (1,3-dicyclohexyl urea) was removed by filtration. The filtrate was then rotary evaporated to dryness, redissolved in dichloromethane (25ml) and chromatograph on silica gel (350g), eluting with dichloromethane (1500ml) and collecting 25ml fractions. Pyrocoll eluted from the column in fractions 30 through 48. These fractions were then pooled and rotary evaporated to dryness. The residue was re-dissolved in a 50:50 mixture of dichloromethane and hexane and crystals of pyrocoll were obtained after 3 days at -20^{0}C. The crystals were then filtered and dried under vacuum. ^{1}H NMR and X-ray crystallography were used to confirm the chemical structure of pyrocoll.

Establishing that pyrocoll interacts with sulfhydryl (SH) groups on RyR2. To establish that pyrocoll indeed interacts with SH groups on RyR2 [^{3}H]ryanodine binding assays were carried with and without reduced glutathione (1000µM) in the binding buffer. The underlying assumption here was that since the concentration of SH groups provided by reduced glutathione is much greater than the molar sum of the free SH groups on RyR2, then if pyrocoll is indeed reacting with SH groups, reduced glutathione should blunt its effects. For this, 100µg/ml vesicle protein from control rat hearts was incubated in binding buffer (500mM KCl, 20mM Tris.HCl and 300µM $CaCl_2$, 0.1mM EGTA, 6.7nM [^{3}H]ryanodine, pH 7.4) for 2 hr at 37^{0}C with increasing concentrations of

pyrocoll (0.5 to 80μM). After incubation, the vesicles were filtered, washed and the amount of [^{3}H]ryanodine bound to RyR2 was determined by liquid scintillation counting. Binding assays were also performed as described above with the inclusion of 1000μM reduced gluthathione in the binding buffer. Non-specific binding was determined by incubating vesicles with 1μM unlabeled ryanodine.

Probing SH groups on RyR2 that are oxidized by diabetes. For this, 100μg/ml membrane vesicle protein from 6-week control, 6-week STZ-diabetic, and 4-week STZ-induced diabetic/2-week insulin treated rat hearts were incubated in binding buffer (500mM KCl, 20mM Tris.HCl and 300μM $CaCl_2$, 0.1mM EGTA, 6.7nM [^{3}H]ryanodine, pH 7.4) for 2 hr at 37^{0}C with increasing concentrations of pyrocoll (0.5 to 80μM). Non-specific binding was determined simultaneously by co-incubating membrane vesicles with 1μM unlabeled ryanodine. After incubation, vesicles were filtered, washed and the amount of [^{3}H]ryanodine bound to RyR2 was determined by liquid scintillation counting.

Data analysis and statistics. Differences between values from each of control, STZ-induced and insulin-treated diabetic rats were evaluated using analysis of variance (ANOVA) followed by Neuman-Keul's test. The data shown are means ± standard errors of means (S.E.M). Results were considered significantly different if $p < 0.05$.

Results

Induction of experimental STZ-induced diabetes mellitus: Mean body weight of all animals at the start of the study was 185.3 ± 2.1g (188.3 ± 2.7g for control animals and 182.6 ± 1.6g for STZ-diabetic animals). As shown in Figure 2, after 42 days the mean body weight of animals injected with citrate buffer only (controls) increased to 386.8 ± 2.1g while the mean body weight of animals injected with 50mg/kg streptozotocin increased only minimally (from 188.1 ± 1.5 to 200.7 ± 9.2 grams). With insulin treatment, body mass of STZ-diabetic animals returned sharply during the subsequent two-week period. Similarly, at the beginning of the study the average glucose level of all animals was 4.1 ± 0.2mM (3.8 ± 0.3 for control animals and 4.4 ± 0.1 for STZ diabetic animals). For those animals injected with citrate buffer only, mean blood glucose levels did not change significantly throughout the 42-day study (4.3 ± 0.2mM at time of sacrifice). However, the blood glucose levels of animals injected with 50mg/kg STZ increased to 20.8 ± 0.7mM after 3 days and increased progressively thereafter to 28.6 ± 1.4mM by day 42. Two weeks of insulin treatment initiated after 4-weeks of untreated diabetes, returned both body weights and blood glucose levels to near control values. Some other characteristics of the animals used in this study are also listed in Table 1.

Quantitation of mRNA encoding RyR2 from control, STZ-diabetic and insulin-treated rat hearts:

mRNA encoding RyR2 was quantitated using reverse transcription-polymerase chain reactions employing β-actin as the internal reference. As shown in Figure 3, after normalizing to concomitant β-actin, mRNA encoding RyR2 did not change significantly

after 6-weeks of diabetes when compared with age-matched controls (99.3 ± 0.4% of control). Also, the amounts of mRNA encoding RyR2 from 4-week STZ diabetic/2-week insulin-treated rat hearts were not significantly different from age-matched controls (106.0 ± 7.2% of controls, $p > 0.05$). It should be pointed out that in these experiments, the amount of mRNA encoding β-actin in control, STZ-induced diabetic and insulin-treated rat hearts were also not significantly different.

Determination of the amount of RyR2 protein in control, STZ-diabetic and insulin-treated rat hearts: One hundred microgram (100μg) of membrane vesicles from 6-week STZ-induced diabetic, 4-week STZ-induced diabetic/2-week insulin-treated and age-matched control rat hearts were solubilized and electrophoresed using 4-20 % linear gradient SDS-polyacrylamide gels. The intensities of RyR2 protein bands were then interpolated on RyR2 calibration curves (run simultaneously on the same gels) to determine RyR2 mass content (Figures 4A and 4B). Using this method, hearts from 6-week STZ-induced diabetic, 4-week STZ-induced diabetic/2-week insulin-treated and age-matched controls contained 280.2 ± 22.7, 313.0 ± 35.6 and 302.2 ± 34.4ng of RyR2/100μg of membrane vesicles, respectively. These mean values were not significantly different. Western blot analyses were carried out to confirm these data. As shown in Figure 5, when normalized to concomitant β-actin content, the amount of immuno-reactive RyR2 protein in control, 6-week STZ-induced and 4-week STZ-diabetic/2-week insulin-treated diabetic rat hearts were not significantly different (100.0 ± 5.3%, 99.42 ± 4.5% and 94.7 ± 5.6% respectively, $p > 0.05$). These data are consistent with our previous studies (Bidasee et al., 2001, 2002).

JPET Fast Forward. Published on February 20, 2003 as DOI: 10.1124/jpet.102.046201
This article has not been copyedited and formatted. The final version may differ from this version.

Ability of RyR2 from control, STZ-diabetic and insulin-treated rat hearts to bind [^{3}H]ryanodine. As shown in Figure 6A, 100µg of membrane vesicles from 6-week STZ-diabetic animals bound 36.7 % less [^{3}H]ryanodine than that from age-matched controls (49.2 ± 7.2 compared with 77.8 ± 5.1 fmol [^{3}H]ryanodine/100µg of membrane vesicles). On the other hand, 100µg of membrane vesicles from insulin-treated animals bound 14.8% more [^{3}H]ryanodine than age-matched controls (89.3 ± 11.9 fmol [^{3}H]ryanodine/100µg of membrane vesicles). Since the RyR2 content varied from preparation to, the amount of [^{3}H]ryanodine bound was normalized to a fixed concentration of RyR2 protein. As shown in Figure 6B, when normalized per µg of protein, RyR2 from 6-week STZ-induced diabetic animals bound 43.3% less [^{3}H]ryanodine when compared to age-matched controls (157.3 ± 22.8 *vs* 277.8 ± 17.8 fmol [^{3}H]ryanodine/µg RyR2, $p < 0.05$) while RyR2 from insulin-treated animals bound 6.4% more than controls (295.5 ± 39.4 fmol [^{3}H]ryanodine/µg RyR2). The latter was not significantly different from controls.

Affinity of RyR2 from control, STZ-diabetic and insulin-treated rat hearts for ryanodine: Equilibrium displacement binding assays were also used to determine the affinity of RyR2 for ryanodine. As shown in Figure 7, IC_{50} values for ryanodine were not significantly different between RyR2 from control, STZ-diabetic and insulin-treated rat

hearts (4.3 ± 0.2, 4.5 ± 0.2 and 5.9 ± 0.1nM, respectively). However, the displacement curve for RyR2 from insulin-treated animals is shifted slightly to the right of those from control and STZ-induced diabetic rat hearts. Using the Cheng-Prusoff equation, the K_d values for ryanodine were also calculated (K_L, the equilibrium dissociation constant for [^{3}H]ryanodine is 1.2nM). The K_d values among the different experimental groups were also not significantly different (0.7 ± 0.1, 0.7 ± 0.1, and 0.9 ± 0.1nM for RyR2 from control, STZ-diabetic and insulin-treated animals, respectively, see Figure 7). Similar to our previous findings (Bidasee et al., 2001, 2002), data from the present study show that diabetes decreases the B_{max} of RyR2 for ryanodine but the K_d of ryanodine remains essentially changed.

Effect of diabetes on the oxidative state of SH groups on RyR2: If oxidative stress is increased with diabetes, then it is likely that SH groups on cysteine residues are oxidized and some adjacent cysteine residues may form disulfide bonds. If so, then breaking these additional disulfide bonds should restore RyR2 ability to bind [^{3}H]ryanodine. As shown in Figure 8, *in vitro* treatment of RyR2 from control animals with 2mM dithiothreitol increased it ability to bind [^{3}H]ryanodine by 16.3 ± 1.3 % ([^{3}H]ryanodine binding increased from 277.7 ± 2.1 to 323.0 ± 3.2 fmol [^{3}H]ryanodine/µg RyR2). On the other hand, *in vitro* treatment of RyR2 from 6-week STZ diabetic rat hearts with 2mM dithiothreitol increased its ability to bind [^{3}H]ryanodine by more than 60% (from 147.6 ± 2.0 to 237.4 ± 0.6 fmol [^{3}H]ryanodine/µg RyR2). Thus, 2mM

dithiothreitol is able to normalize [^{3}H]ryanodine binding to that of untreated controls. *In vitro* treatment of RyR2 from control animals with 500µM dithiothreitol for 2hr at 37^{0}C decreased its ability to bind [^{3}H]ryanodine by 12.9 ± 2.3 % (from 277.7 ± 2.1 to 242.0 ± 3.6 fmol [^{3}H]ryanodine per µg RyR2), Figure 8. Interestingly, this treatment increases [^{3}H]ryanodine binding to RyR2 from STZ-diabetic animals by 30.6 ± 2.1% (from 147.6 ± 2.0 to 192.3 ± 2.4 fmol [^{3}H]ryanodine/µg RyR2). These data are consistent with the notion that the decreased ability of RyR2 from 6 week diabetics to bind [^{3}H]ryanodine stems at least in part from diabetes-induced increases in its disulfide bond content.

Synthesis of the pyrrole-containing sulfhydryl reagent pyrocoll (5H,10H-dipyrrolo[1,2-a:1',2'-d]pyrazine-5,10-dione): In this study the ketene pathway was utilized for synthesis of pyrocoll (Qiao et al., 1996, refer to Figure 1). Yields of pyrocoll after purifying and crystallizing typically ranged between 1.5 and 2% (≈ 15 to 20 mg). This low yield is consistent with the notion that pyrocoll was formed not as the major, but a side product of the reaction.

Establishing that pyrocoll interacts with sulfhydryl groups on RyR2: As indicated above, although pyrocoll has the pre-requisites of a sulfhydryl interacting reagent, this property has not been experimentally demonstrated. As shown in Figure 9(●), when RyR2 from control animals were treated with 0.5µM pyrocoll, [^{3}H]ryanodine binding decreased by 9.8 ± 2.3% (indicative of channel deactivation). Increasing the

concentration of pyrocoll to 1μM further decreased [^{3}H]ryanodine binding by 16.6 ± 2.3%. At a concentration of 5μM, the ability of pyrocoll to decrease [^{3}H]ryanodine binding was diminished to 9.5 ± 2.2%. Thereafter, concentrations of pyrocoll (≥ 10μM) increased [^{3}H]ryanodine binding to RyR2 in a concentration-dependent manner (up to 9.8 ± 1.4% with 25μM). Co-incubation with 1mM reduced glutathione, blunts both effects of pyrocoll (Figure 9(○)). Since at this concentration, reduced glutathione does not have significant effects on the binding of [^{3}H]ryanodine to RyR2 (data not shown), these data strongly suggest that the pyrrole containing quinone alters the activity of RyR2 by interacting with free SH groups.

Characterizing the SH groups on RyR2 that are oxidized by diabetes: Since RyR2 contains two distinct classes of pyrocoll-sensitive cysteine residues, experiments were conducted to determine which of these classes of cysteines are affected by diabetes. As shown in Figure 10(●), when RyR2 from control animals were treated with pyrocoll, the two expected effects were observed, i.e., up to concentrations of 1μM, it inhibited the binding of [^{3}H]ryanodine to RyR2, consistent whit channel deactivation, while at concentrations above that it increased [^{3}H]ryanodine binding (channel activation). Treatment of RyR2 from 6 week diabetic animals with pyrocoll (up to 1μM) resulted in typical inhibition of [^{3}H]ryanodine binding (19.9 ± 0.1%). However, treatment with higher concentrations of pyrocoll (up to 80μM), did not trigger the typical increase [^{3}H]ryanodine binding.

As with RyR2 from control and STZ-diabetic animals, treatment of RyR2 from insulin-treated animals with low concentrations of pyrocoll (up to 1µM) also resulted in decrease in [^{3}H]ryanodine binding. However, at higher concentrations (up to 80µM), pyrocoll was not able to fully increase RyR2 bind of [^{3}H]ryanodine (37.5% of the maximum response elicited by RyR2 from control animals). These data suggest that 2-weeks of insulin-treatment is able to partially prevent/minimize the loss in [^{3}H]ryanodine binding induced by diabetes. These data are consistent with our prior study (Bidasee et al., 2001) as well as that of Netticadan et al., (2001).

Discussion

Although diabetic pathology progression can be delayed with combinations of insulin replacement therapy, drugs, diet and exercise, a significant number of chronic diabetic patients eventually develop cardiac failure, attributable to systolic dysfunction. Using animal models of the syndrome, studies have shown that dysfunction results from changes in expression and/or function of several key proteins involved in regulating/maintaining intracellular calcium homeostasis (Tahiliani and McNeill, 1986; Takeda et al., 1996). One of these proteins is the type 2 ryanodine receptor calcium-release channel (RyR2); the channel through which calcium ions leave the sarcoplasmic reticulum to trigger cardiac contraction. Using the STZ-induced diabetic rat model, we recently showed that after 6-weeks of diabetes, expression of RyR2 did not change (Bidasee et al., 2001). However, its activity as assessed from its ability to bind [^{3}H]ryanodine, had become compromised. This study is part of a series of experiments designed to elucidate the mechanism(s) underlying RyR2 dysfunction in diabetes.

The principal finding of the present study is that the loss in activity of RyR2 in diabetes stems in part from an increase in its disulfide bond (S-S) content. This conclusion is based on our finding that when RyR2 from 6 week diabetic animals was treated with a reducing concentration of dithiothreitol (2mM), its ability to bind [^{3}H]ryanodine was restored to near control values. It should be pointed out that the severe diabetes characterizing our STZ model undoubtedly represents multifactorial pathologies that contribute to overall oxidative stress; our results should not be construed to represent the effects of hyperglycemia alone. Further, we must acknowledge that the results could also be due to the severely stunted growth of the

rats, rather than hyperglycemia alone. This discovery raises several interesting questions, one of which is "how many of ≈ 84 free thiols (≈ 21 per monomer) on RyR2 are modified by diabetes?" What we do know to date is that oxidation of up to 12 (presumably the most reactive) of these SH residues increases activity of RyR2 (opens the channel), whereas oxidation of greater than 24 decreases channel activity (closes the channel, Xu et al., 1998). Since the binding of [^{3}H]ryanodine to RyR2 decreases with diabetes and it is likely that up to 24 of the 84 free thiols on RyR2 may be modified by diabetes. Exactly where these sulfhydryl groups are located on RyR2 remains to be elucidated.

Functional ryanodine receptors are made up of four monomers (homo- or hetero-tetrameric, Xiao et al., 2002) held together by strong electrostatic interactions and possibly inter monomer disulfide bonds. Thus, another obvious question that arises from this study is "what fraction of these additional disulfide bonds is formed intra- and what fraction is formed inter-monomers?" In an attempt to address this question, the electrophoretic profile of diabetic RyR2 that has been treated with dithiothreitol was compared with that of RyR2 from diabetic and age-matched controls. The underlying assumption here is that if additional inter- or intra-monomer disulfide bonds are being formed, then the electrophoretic mobility of RyR2 from diabetic animals will be altered and such a change should be reversed by treating with dithiothreitol. In preliminary experiments, we did find that the electrophoretic mobility of RyR2 from STZ-diabetic rats was slower than RyR2 from control rats (Bidasee et al., 2002). However, the shift was too small to be attributed to "dimer" formation. Thus, from these preliminary

experiments, it is likely that intra-monomer rather than inter-monomer disulfide bonds are being formed on RyR2.

Studies have shown that several classes of reactive sulfhydryl groups exist on RyR2 (Agdhasi et al., 1997; Eager et al., 1997; Xu et al., 1998; Salama et al., 2000; Sun et al., 2001). Most reagents tested exhibit two distinct and opposing effects on binding to these SH groups. At lower concentrations they increase the activity of RyR2 (increase [^{3}H]ryanodine binding), while at higher concentrations or longer exposure times, they deactivate or close the channel (seen as a decrease in [^{3}H]ryanodine binding). In this study, we synthesized and tested a targeted sulfhydryl reagent, namely pyrocoll. As predicted, this compound also increased and decreased channel activity. However, unlike most sulfhydryl reagents, it first deactivated and then activated RyR2. Thus, pyrocoll appears to be similar to the sulfhydryl reagent N-ethylmaleimide, which is also alkylating (Aghdasi et al., 1997), with the exception that it is substantially more potent: only nanomolar concentrations are required for its effects. At this time we are not certain whether pyrocoll also has alkylating properties.

Another major finding of the present study is that after 6-weeks of diabetes, pyrocoll-sensitive SH groups that activate RyR2 (trigger increases in [^{3}H]ryanodine binding) are no longer available for interactions. Two reasons can be envisioned for this. First the class of SH groups triggering channel activation might have been oxidized by diabetes and therefore no longer available for interaction with pyrocoll. Alternatively, it is possible that diabetes can induce modifications at distal sites resulting

in sufficient conformation change to prevent pyrocoll from interacting with the class of SH groups that triggers channel activation.

In this study we found that two weeks of insulin-treatment was able to partially but not fully restore binding of [^{3}H]ryanodine to RyR2. These data suggest that either the turnover rate of RyR2 is slow (more than 14 days is needed to completely turn over protein) or that modifications other than disulfide bond formation are being induced by diabetes. Not all of the available free SH groups on cysteine residues will be oxidized to form disulfide bonds. Some of the SH groups will react with oxygen species to form sulfenic acid derivative (cys-S-OH) while others may react with nitrogen species to form S-nitroso-cysteines. In addition, other amino acid residues are also capable of undergoing oxidative modification. Studies have shown that histidine residues can also be oxidized to form 2-oxohistidine, tryptophan residues can be oxidized to kynurenine/n-alkylkynurenine, methionine residues can be oxidized to form methionine sulfoxide/sulfone, and that tyrosine, leucine and valine residues can also be modified to form their dihydroxy and hydroxy derivatives, to name a few (Stadtman and Levine, 2000; Droge, 2002). Modification of these amino acids, especially those that are exposed may be sufficient to induce enough of a conformation change on the RyR2 such that the net effect is channel deactivation. In a recent study, Netticadan et al., (2001) showed that phosphorylation of RyR2 by Ca^{2+}-calmodulin dependent- and cAMP dependent-protein kinases increases in diabetes suggesting that oxidative modifications of tyrosine, serine and threonine may be occurring only minimally.

Lysine, arginine, cysteine and histidine residues on RyR2 can also react non-enzymatically with aldose and ketose sugars to form Schiff bases. On long-lived

proteins these Schiff bases can undergo internal rearrangement to form Amadori products. Through a series of rearrangement, dehydration, oxidation, condensation, elimination and cyclization reactions, these Amadori products can rearrange further to form advanced-glycation end products (AGEs). In preliminary experiments, when membrane vesicles from 6-week STZ-diabetic animals were excited with ultraviolet light at 350nm, emission spectra typical of AGEs were observed (λ_{max} between 400nm and 450nm, see Figure 11). This fluorescence was not detected in vesicles prepared from age-matched controls. It should be pointed out that these data represent the aggregate fluorescence on all long-lived proteins in membrane vesicle preparations. We are in the process of determining whether AGEs are formed on RyR2.

In conclusion, data from the present study show that STZ-induced diabetes increases disulfide bond formation on RyR2 and decreases ligand binding, thus suggesting that the channel is stabilized in the closed conformation. As such, the ability of RyR2 from 6-week STZ-diabetic rat hearts to bind [^{3}H]ryanodine decreases as this ligand binds within the pore-forming segment of the channel. Our data also show that these changes could be minimized but not fully restored with 2-weeks of insulin treatment, initiated after 4-weeks of untreated diabetes. Could the decreased ability of RyR2 to bind [^{3}H]ryanodine in the ischemic model of heart failure (Darling et al., 1992; Holmberg and Williams, 1992) be due to increased disulfide formation (induced by an oxidative cellular environment)? If so, then perhaps disulfide bond formation on RyR2 may serve as a protective mechanism against intracellular calcium overload.

Acknowledgements

The authors thank Yongqi Yu for valuable technical assistance and Dr. John C. Huffman Molecular Structure Center, Department of Chemistry, Indiana University at Bloomington, for crystal structure of pyrocoll.

References

Aghdasi B, Zhang JZ, Wu Y, Reid MB and Hamilton SL (1997) Multiple classes of sulfhydryls modulate the skeletal muscle Ca^{2+} release channel. *J Biol Chem* **272**:3739-3748.

Anzai K, Ogawa K, Kuniyasu A, Ozawa T, Yamamoto H and Nakayama H (1998) Effects of hydroxyl radical and sulfhydryl reagents on the open probability of the purified cardiac ryanodine receptor channel incorporated into planar lipid bilayers. *Biochem Biophys Res Commun* **249**:938-942.

Asmal AC, Leary WP and Thandroyen FS (1980) Diabetic heart disease. *Afr Med J* **57**:788-790.

Baynes JW, Watkins NG, Fisher CI, Hull CJ, Patrick JS, Ahmed MU, Dunn JA and Thorpe SR (1989) The Amadori product on protein: structure and reactions. *Prog Clin Biol Res* **304**:43-67.

Bidasee KR and Besch HR Jr (1998) Structure-function relationships among ryanodine derivatives. Pyridyl ryanodine definitively separates activation potency from high affinity. *J Biol Chem* **273**:12176-12186.

Bidasee KR, Dincer UD and Besch HR Jr (2001) Ryanodine receptor dysfunction in hearts of streptozotocin-induced diabetic rats. *Mol Pharmacol* **60**:1356-1364.

Bidasee KR, Nallani K, Henry B, Dincer UD and Besch HR Jr (2002), Chronic diabetes alters function and expression of ryanodine receptor calcium-release channels in rat hearts. *Mol Cell Biochem* (in press, 2003).

Brownlee M, Cerami A and Vlassara H (1988) Advanced glycosylation end products in tissues and the biochemical basis of diabetic complications. *N Engl J Med* **319**:315-321.

Bucala R and Cerami A (1992) Advanced glycosylation, Chemistry, biology and implications for diabetes and aging. *Adv Pharmacol* **23**:1-34.

Darling E, Lai RA, Meissner G (1992) Effects of regional ischemia on ryanodine – sensitive Ca2+ release channel of canine cardiac sarcoplasmic reticulum. *J Mol Cell Cardiol* **24:**1179-1188.

Dhalla NS, Temsah RM and Netticadan T (2000) Role of oxidative stress in cardiovascular diseases. *J Hypertens* **18**:655-673.

Droge W (2002) Free radicals in the physiological control of cell function. *Physiol Rev* **82**:47-95.

Eager KR, Roden LD and Dulhunty AF (1997) Actions of sulfhydryl reagents on single ryanodine receptor Ca^{2+}-release channels from sheep myocardium. *Am J Physiol* **272**:C1908-1918.

Evans JL, Goldfine RD, Maddux BA and Grodsky GM (2002) Oxidative stress and stress-activated signaling pathways: A unifying hypothesis of type 2 diabetes. *Endo Reviews* **23**:599-622.

Fein FS (1990) Diabetic Cardiomyopathy. *Diabetes Care* **13(Supp 4)**: 1169-1179.

Feng W, Liu G, Xia R, Abramson JJ and Pessah IN (1999) Site-selective modification of hyperreactive cysteines of ryanodine receptor complex by quinones. *Mol Pharmacol* **55**:821-831.

Hamby RI, Zoneraich S and Sherman S (1974) Diabetic cardiomyopathy. *JAMA* **229**:1749-1754.

Holmberg SRM, Williams AJ (1992) The calcium release channel from cardiac sarcoplasmic reticulum. Function in failing and acute ischemic heart. *Basic Res Cardiol* **87:**255-268.

Janka HU (1996) Increased cardiovascular morbidity and mortality in diabetes mellitus: identification of the high risk patient. *Diabetes Res Clin Pract* **30 (Suppl)**:85-88.

Koistinen MJ (1990) Prevalence of asymptomatic myocardial ischaemia in diabetic subjects *Brit Med J*. **301**:92-95.

Liu G, Abramson JJ, Zable AC and Pessah IN (1994) Direct evidence for the existence and functional role of hyperreactive sulfhydryls on the ryanodine receptor-triadin complex selectively labeled by the coumarin maleimide 7-diethylamino-3-(4'-maleimidylphenyl)-4-methylcoumarin. *Mol Pharmacol* **45**:189-200..

Netticadan T, Temsah RM, Kent A, Elimban V and Dhalla NS (2001) Depressed levels of Ca^{2+}-cycling proteins may underlie sarcoplasmic reticulum dysfunction in the diabetic heart. *Diabetes* 2001 **50**:2133-2138.

Qiao GGH, Andraos J and Wentrup C (1996) Reactivity of ketenes in matrixes. Direct observation of ketene-pyridine ylides. *J Am Chem Soc* **118**: 5634-5638.

Rodrigues B, Cam MC and McNeill JH (1998) Metabolic disturbances in diabetic cardiomyopathy. *Mol Cell Biochem* **180**:53-57.

Rubler S, Dlugash J, Yuceoglu YZ, Kumral T, Branwood AW and Grishman A (1972) New type of cardiomyopathy associated with diabetic glomerulo-sclerosis. *Am J Cardiol* **30**:595-560.

Salama G, Menshikova EV and Abramson JJ (2000) Molecular interaction between nitric oxide and ryanodine receptors of skeletal and cardiac sarcoplasmic reticulum. *Antioxid Redox Signal* **2**:5-16.

Stadtman ER and Levine RL (2000) Protein oxidation. *Ann N Y Acad Sci* **899**:191-208.

Sun J, Xu L, Eu JP, Stamler JS and Meissner G (2001) Classes of thiols that influence the activity of the skeletal muscle calcium release channel. *J Biol Chem* **276**:15625-15630.

Tahiliani AG and McNeill JH (1986) Diabetes-induced abnormalities in the myocardium. *Life Sci* **38**:959-974.

Takeda N, Dixon IM, Hata T, Elimban V, Shah KR and Dhalla NS (1996) Sequence of alterations in subcellular organelles during the development of heart dysfunction in diabetes. *Diabetes Res Clin Pract* **30 (Suppl)**:113-122.

Teshima Y, Takahashi N, Saikawa T, Hara M, Yasunaga S, Hidaka S and Sakata T (2000) Diminished expression of sarcoplasmic reticulum Ca(2+)-ATPase and ryanodine sensitive Ca(2+) channel mRNA in streptozotocin-induced diabetic rat heart. *J Mol Cell Cardiol* **32(4):**655-664.

Trimm JL, Salama G and Abramson JJ (1986) Sulfhydryl oxidation induces rapid calcium release from sarcoplasmic reticulum vesicles. *J Biol Chem* **261**:16092-16098.

Weis M, Morgenstern R, Cotgreave IA, Nelson SD and Moldeus P (1992) N-acetyl-p-benzoquinone imine-induced protein thiol modification in isolated rat hepatocytes. *Biochem Pharmacol* **43**:1493-1505.

Welch W, Sutko JL, Mitchell KE, Airey J and Ruest L (1996) The pyrrole locus is the major orienting factor in ryanodine binding. *Biochem* **35**:7165-7173.

Wolff SP, Jiang ZY and Hunt JV (1991) Protein glycation and oxidative stress in diabetes mellitus and ageing. *Free Radic Biol Med* **10**:339-352.

Xiao B, Masumiya H, Jiang D, Wang R, Sei Y, Zhang L, Murayama T, Ogawa Y, Lai FA, Wagenknecht T and Chen SR (2002) Isoform dependent formation of heteromeric Ca2+ release channels (ryanodine receptors). *J Biol Chem* **277**:41778-41785

Xu L, Eu JP, Meissner G and Stamler JS (1998) Activation of the cardiac calcium release channel (ryanodine receptor) by poly-S-nitrosylation *Science* **279**:234-237.

Yu Z and McNeill JH (1991) Force-interval relationship and its response to ryanodine in streptozotocin-induced diabetic rats. *Can J Physiol Pharmacol* **69(9)**:1268-1276.

Yu Z, Tibbits GF and McNeill JH (1994) Cellular functions of diabetic cardiomyocytes: contractility, rapid-cooling contracture, and ryanodine binding. *Am J Physiol* **266**:H2082-2089.

Zhong Y, Ahmed S, Grupp IL and Matlib MA (2001) Altered SR protein expression associated with contractile dysfunction in diabetic rat hearts. *Am J Physiol* 281:H1137-1147.

Footnotes:

(a) This work was supported in part by grants from the National Institutes of Health (RO1-HL66898) and the Ralph W. and Grace M. Showalter Trust.

(b) Address request for reprints to:

Keshore R. Bidasee, Ph.D. Associate Professor Department of Pharmacology, PYH 5006 University of Nebraska Medical Center 986260 Nebraska Medical Center Omaha, NE 68198-6260

Legend for Figures

Figure 1:

Reaction scheme for synthesis of pyrocoll. Reaction reagents and conditions are described in the text. Configurations shown represent two-dimensional projections using the algorithms of CSC ChemOffice, Version 5 (Cambridge Scientific Computing Inc., Cambridge, MA).

Figure 2:

Average body weight (A) and blood glucose levels of animals during the course of the study. Values shown represent means ± SEM for at least 10 animals in each group

Figure 3:

Relative levels of mRNA encoding RyR2 from 6-week streptozotocin (STZ)-induced, 4-week STZ-induced/2-week insulin-treated diabetic and age-matched control rat hearts. Briefly, total RNA was reverse-transcribed into 1st cDNA using oligo dT_{15} and Superscript II™. Thereafter, specific primers were used in polymerase chain reactions to amplify segments of cDNA encoding RyR2-and β-actin. **A.** (i) Representative sample of PCR products obtained using RyR2 primers; (ii) Signal intensities normalized to concomitant β-actin and relative to those of age-matched controls. **B.** (i) Representative sample of PCR products obtained using β-actin primers; (ii) quantitation of intensities of β-actin signals. Values shown are means ± standard

errors of means (S.E.M.) obtained from 3 individual hearts, analyzed in duplicate. PCR products were of expected sizes: 602bp for RyR2 and 387bp for β-actin.

Figure 4:

Determination of the amount of RyR2 protein present in 100µg of membrane vesicles from 6-week streptozotocin (STZ)-induced, 4-week STZ-induced/2-week insulin-treated diabetic and age-matched control rat hearts. Two steps were used for this**.** Briefly, 100µg of membrane vesicles from each experimental group along with varying concentrations of purified ryanodine receptor (50 to 300ng) were dissolved in gel dissociation medium containing 10mg/ml dithiothreitol and electrophoresed for 3.5hr at 150V using 4-20% linear gradient polyacrylamide gels. The gels were then stained with Coomassie®-dye and de-stained overnight. **(A)** Relative intensities of Coomassie®-stained RyR2 bands from control, diabetic and insulin-treated animals. Values shown are means ± standard errors of means obtained from at least five experiments performed using three different membrane preparations (3 hearts per preparation). **(B)** Example of a RyR2 calibration used for determining amount of protein present in 100µg of membrane vesicles.

Figure 5:

Confirmation of relative levels of RyR2 protein in 100µg of membrane vesicles from 6-week streptozotocin (STZ)-induced, 4-week STZ-induced/2-week insulin-treated diabetic and age-matched control rat hearts. Western blot analyses were used to confirm relative levels of RyR2 protein in 100µg of membrane vesicles from 6-

week streptozotocin (STZ)-induced, 4-week STZ-induced/2-week insulin-treated diabetic and age-matched control rat hearts. For these experiments, β-actin was used as an internal reference to correct for variability in protein load and/or transfer. Values shown are mean ± SEM for three experiments done using three different membrane preparations.

Figure 6:

(A) Amount of [^{3}H]ryanodine bound to 100µg of membrane vesicles from 6-week streptozotocin (STZ)-induced, 4-week STZ-induced/2-week insulin-treated diabetic and age-matched control rat hearts. Briefly, membrane vesicles (0.1mg/ml) from each of control, STZ-induced diabetic and insulin-treated diabetic rat hearts were incubated for 2hr at 37^{0}C with 6.7nM [^{3}H]ryanodine in binding buffer consisting of 500mM KCl, 0.3mM $CaCl_2$, 0.1mM EGTA and 20mM Tris.HCl , (pH 7.4). After incubation, the vesicles were filtered, washed and [^{3}H]ryanodine bound to RyR2 was determined by liquid scintillation counting. Data shown are means ± standard errors of means for at least six experiments done using three different membrane preparations. *denotes significantly different from controls and insulin-treated.

(B) Amount of [^{3}H]ryanodine bound per µg of RyR2 protein from 6-week streptozotocin (STZ)-induced, 4-week STZ-induced/2-week insulin-treated diabetic and age-matched control rat hearts. The amount of RyR2 in 100µg of membrane vesicles was determined by interpolation on RyR2 calibration curves. Then amount [^{3}H]ryanodine bound was normalized to 1µg of RyR2. Values shown are means ±

standard errors of means for at least six experiments done using three different membrane preparations. * denotes significantly different from controls and insulin-treated.

Figure 7:

Measurement of affinities of RyR2 from 6-week streptozotocin (STZ)-induced, 4-week STZ-induced/2-week insulin-treated diabetic and age-matched control rat hearts for ryanodine. Equilibrium dissociation constant (K_d) and IC_{50} values were determined by incubating MV proteins (0.1mg/ml) from 6-week control, 6-week STZ-induced and 4-week STZ-induced diabetic/2-week insulin treated animals for two hr at 37^0C with 6.7nM [^{3}H]ryanodine and increasing concentrations of unlabeled ryanodine up to 300nM. At the end of this time, the vesicles were filtered, washed and [^{3}H]ryanodine bound was determined by liquid scintillation counting. Non-specific binding was simultaneously determined by incubating vesicles with 1μM ryanodine. GraphPad Prism 3.0a was used to drawn curves (non-linear regression) and to calculate IC_{50} values. K_d values were determined using the Cheng-Prusoff equation. Data shown are means for at least six experiments done using three different membrane preparations.

Figure 8:

Effect of dithiothreitol on ability of RyR2 from 6-week streptozotocin (STZ)-induced diabetic and age-matched control rat heart to bind [^{3}H]ryanodine.

Membrane vesicles (0.1mg/ml) from each of control and STZ-induced diabetic were incubated for 2hr at 37^0C with 6.7nM [^{3}H]ryanodine in binding buffer consisting of 500mM KCl, 0.3mM $CaCl_2$, 0.1mM EGTA and 20mM Tris.HCl , (pH 7.4) with either 500µM or 2mM dithiothreitol. After incubation, the vesicles were filtered, washed and [^{3}H]ryanodine bound to RyR2 was determined by liquid scintillation counting. [^{3}H]ryanodine bound was then normalized per µg of RyR2 protein change in [^{3}H]ryanodine bound determine. Data shown are means ± standard errors of means for at least five experiments done three different membrane preparations.

Figure 9:

(A) Ability of reduced glutathione to blunt pyrocoll-induced alterations in [^{3}H]ryanodine binding to RyR2 from control rat hearts. Briefly, membrane vesicles (0.1mg/ml) from control animals were incubated for 2hr at 37^0C with 6.7nM [^{3}H]ryanodine in binding buffer consisting of 500mM KCl, 0.3mM $CaCl_2$, 0.1mM EGTA and 20mM Tris.HCl , (pH 7.4) with varying amount of pyrocoll in the presence or absence of 1mM reduced glutathione. After incubation, the vesicles were filtered washed and [^{3}H]ryanodine bound to RyR2 was determined by liquid scintillation counting. Data shown are means ± standard errors of means for at four experiments done using three different membrane preparations.

Figure 10:

Ability of pyrocoll to modulate the binding of [^{3}H]ryanodine to RyR2 from 6-week streptozotocin (STZ)-induced, 4-week STZ-induced/2-weeks insulin-treated diabetic and age-matched control rat hearts. Membrane vesicles (0.1mg/ml) from each of control, STZ-induced and insulin-treated diabetic rat hearts were incubated for 2hr at 37^{0}C with 6.7nM [^{3}H]ryanodine in binding buffer consisting of 500mM KCl, 0.3mM $CaCl_2$, 0.1mM EGTA and 20mM Tris.HCl , (pH 7.4) with varying concentration of pyrocoll. After incubation, the vesicles were filtered washed and [^{3}H]ryanodine bound to RyR2 was determined by liquid scintillation counting. Data shown are means ± standard errors of means for at least five experiments done using three different membrane preparations. *denote value significantly different from STZ-diabetic, **denote value significantly different from STZ-diabetic.

Figure 11:

Fluorescent scan of membrane vesicles isolated from 6-week age-matched control and 6-week STZ-induced diabetic rat hearts. Briefly, membrane vesicles (0.5mg in 1ml of buffer containing 0.3M sucrose, 10mM imidazole.HCl, 230µM phenylmethyl sulfonyl fluoride (PMSF) and 1.1µM leupeptin, pH 7.4) were excited with 350nm light in a spectrofluorometer (F-2000 Fluorescence Spectrophotometer, Hitachi, Japan). Emission spectra were then monitored between wavelengths 300nm and 600nm. Differences in emission spectra from diabetic preparations may be due to varying amounts of unique advanced-glycation end products present.

JPET Fast Forward. Published on February 20, 2003 as DOI: 10.1124/jpet.102.046201
This article has not been copyedited and formatted. The final version may differ from this version.

Table 1: Some characteristics of animals at the end of the *in vivo* study

Parameter	6-weeks age-matched controls (n = 12)	6-week streptozotocin-induced diabetic (n = 12)	6-week streptozotocin-induced diabetic/2-week insulin-treated (n = 12)
Heart weight (g)	1.1 ± 0.1	0.9 ± 0.2	1.1 ± 0.1
Insulin (ng/ml)	2.2 ± 0.5	0.04 ± 0.02*	4.8 ± 1.5
HbA_{1c} (%)	4.2 ± 0.2	10.8 ± 0.3*	5.9 ± 0.2

Values shown are mean ± standard errors of mean

* significantly different from control and insulin-treated animals

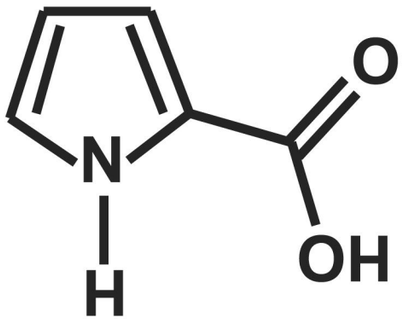

1H-pyrrole-2-carboxylic acid

1,3-dicyclohexylcarbodiimide

in carbon tetrachloride, 2hr at RT

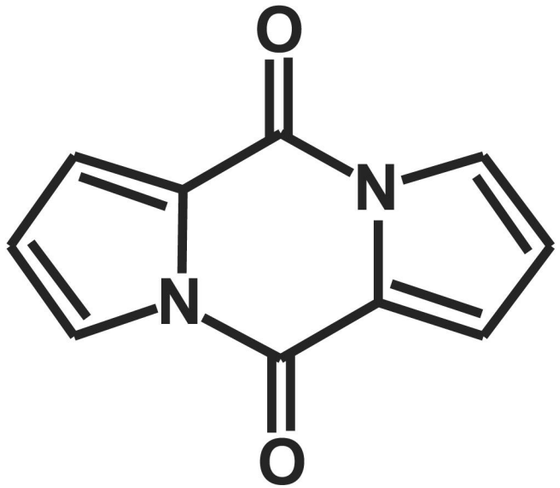

5H, 10H-dipyrrolo[1,2-a;1',2'-d] pyrazine-5,10-dione (Pyrocoll)

Figure 1

A

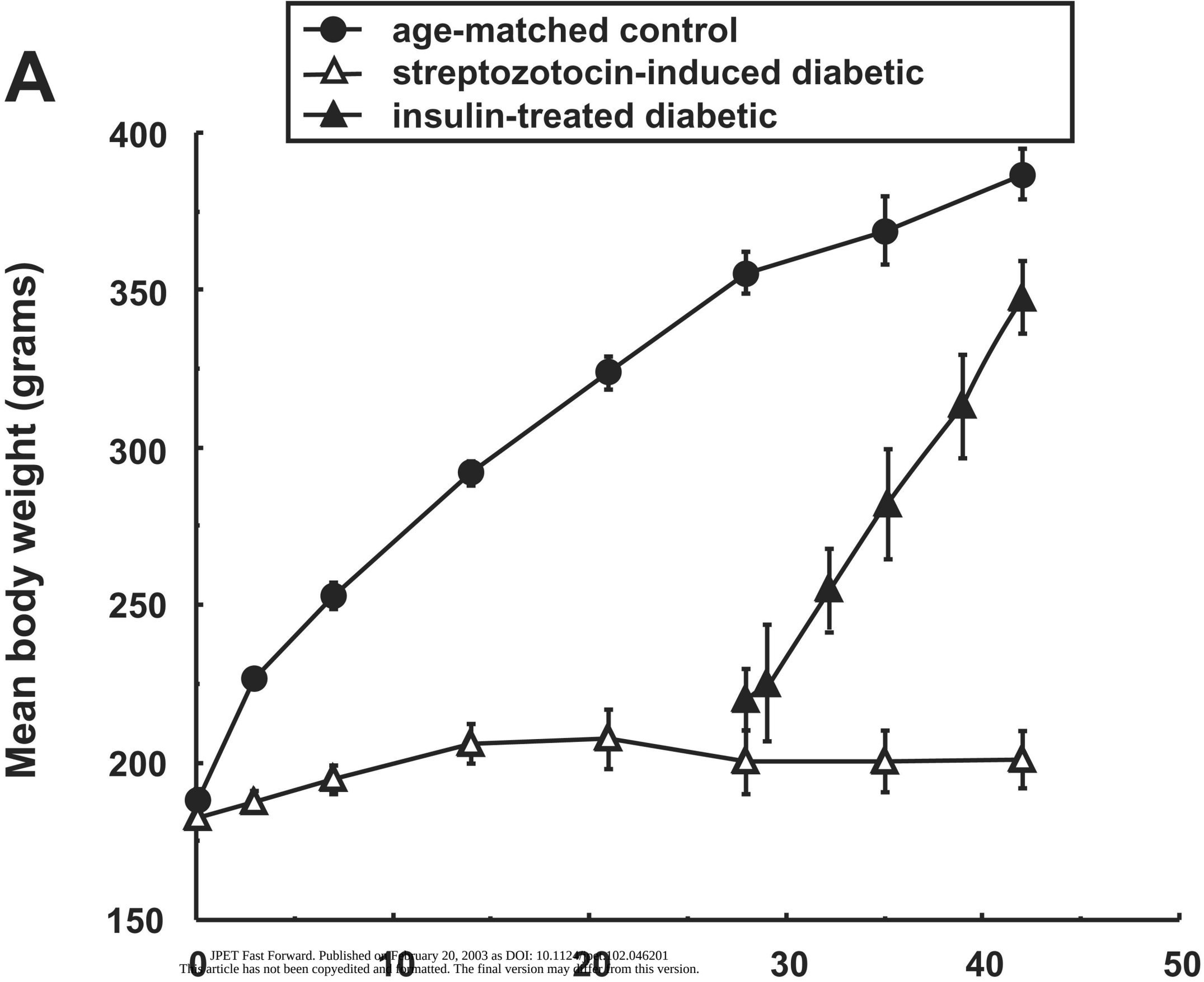

B

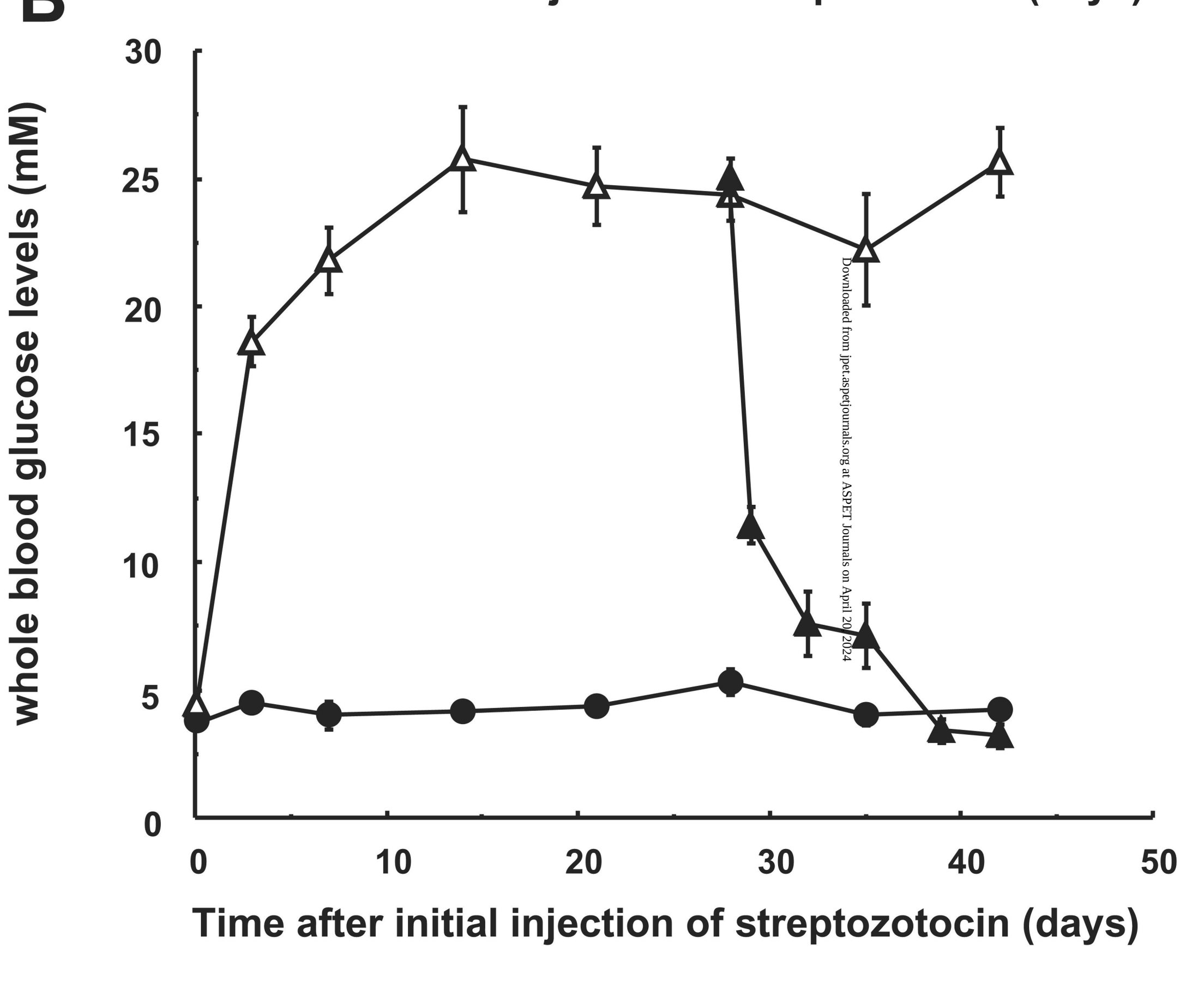

Figure 2

Figure 3

A

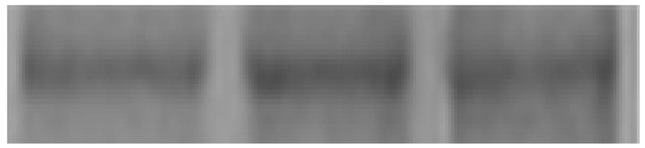

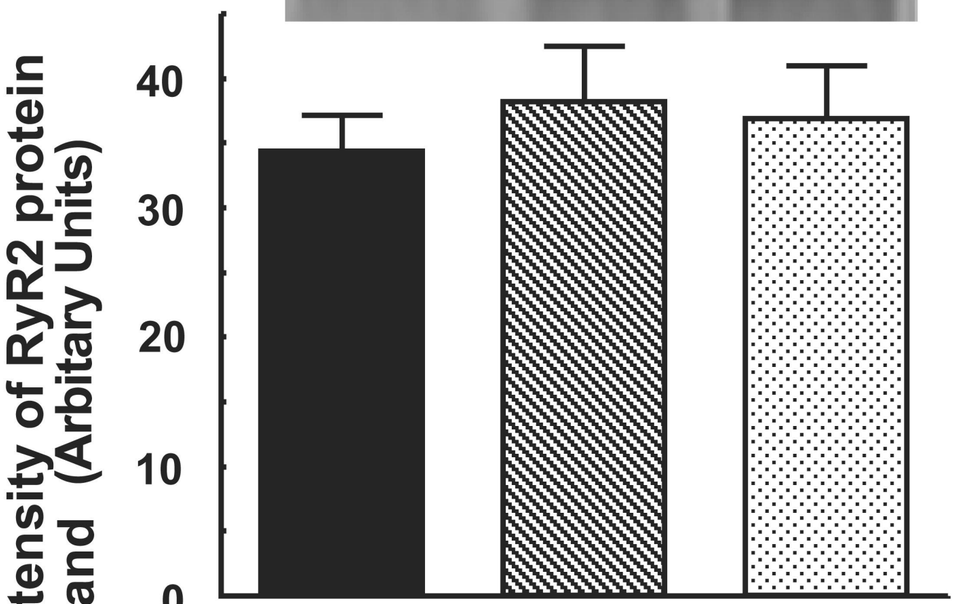

B

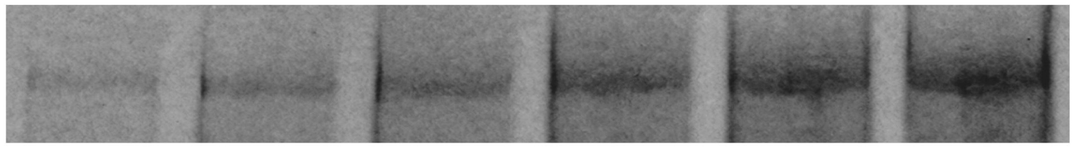

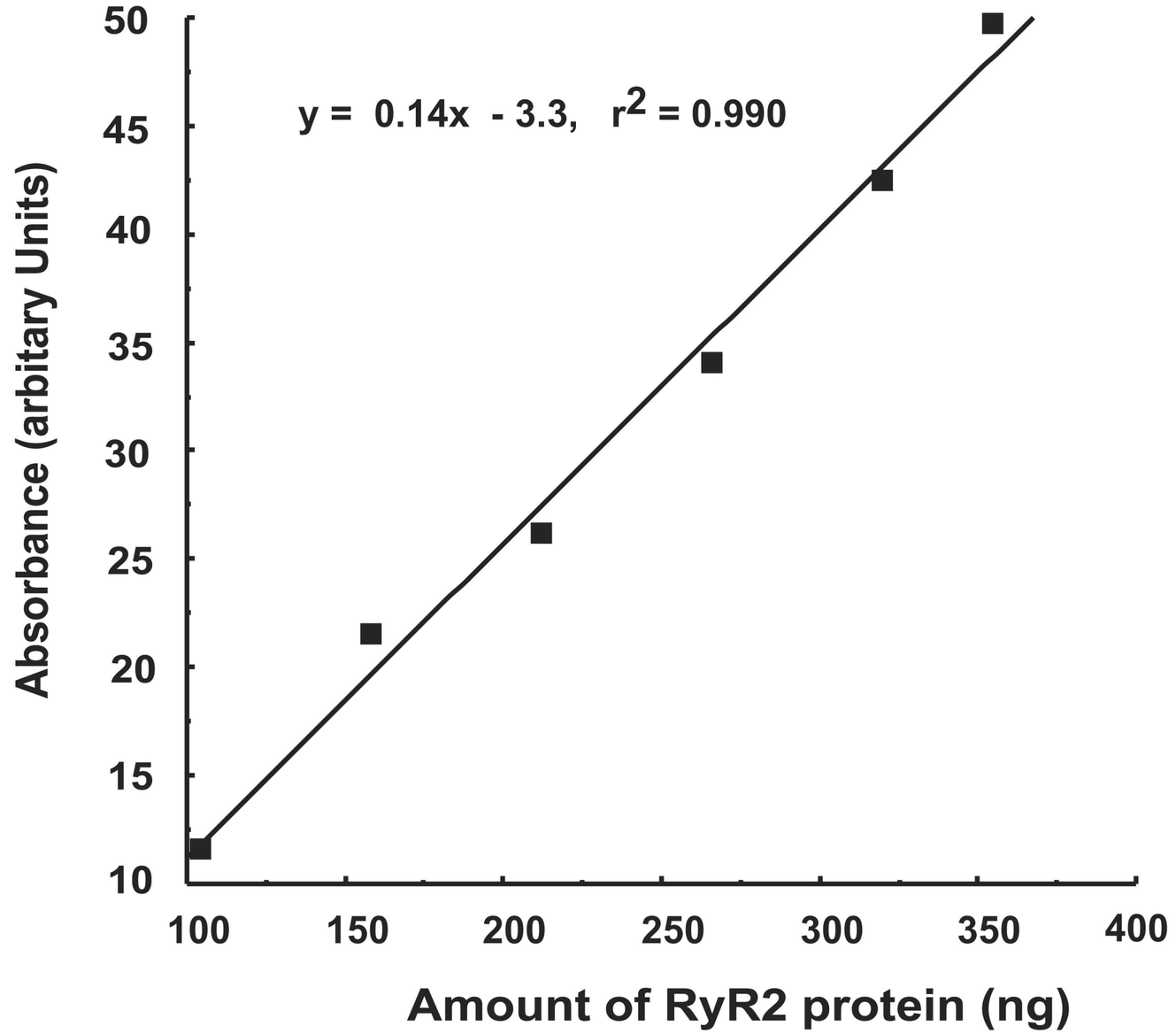

Figure 4

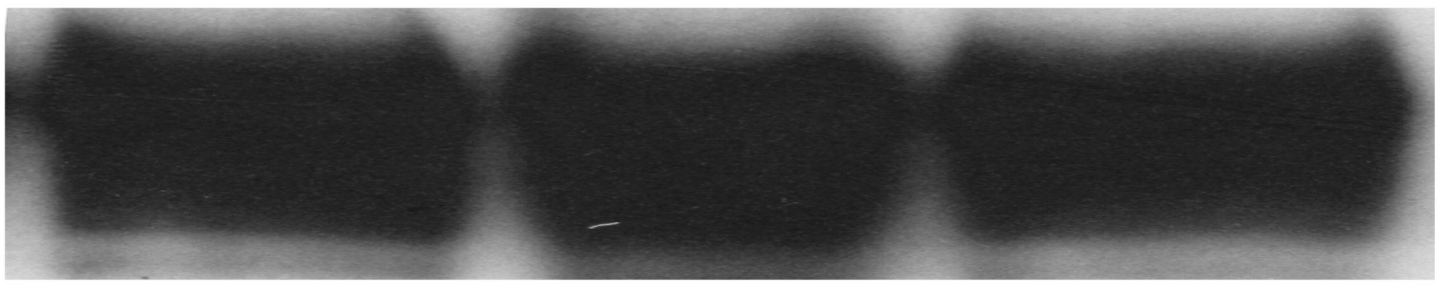

JPET Fast Forward. Published on February 20, 2003 as DOI: 10.1124/jpet.102.046201
This article has not been copyedited and formatted. The final version may differ from this version.

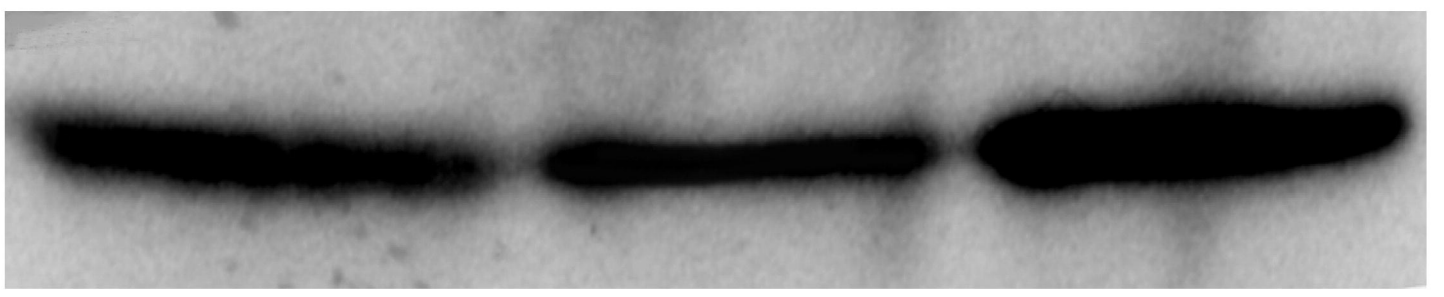

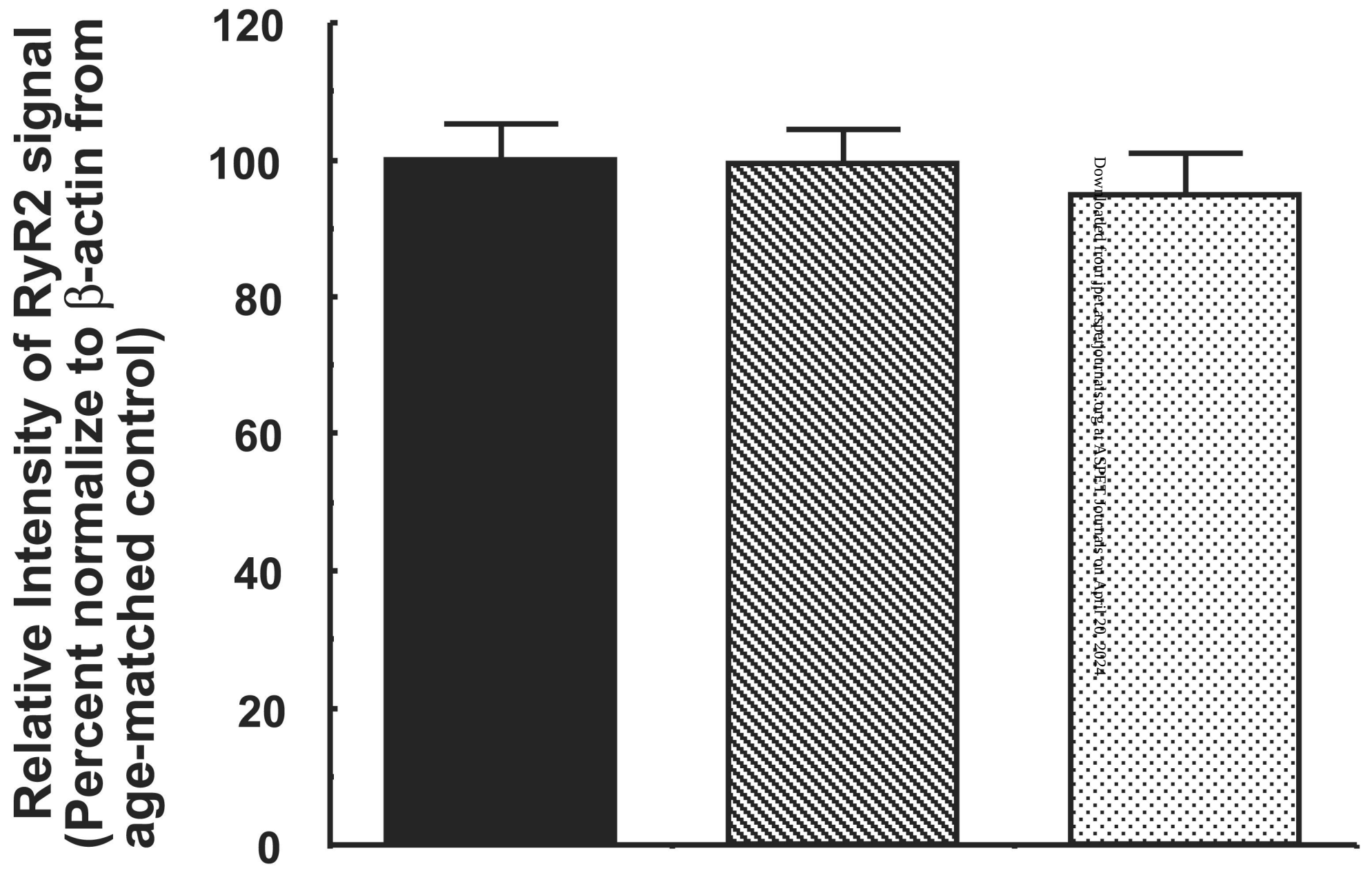

Figure 5

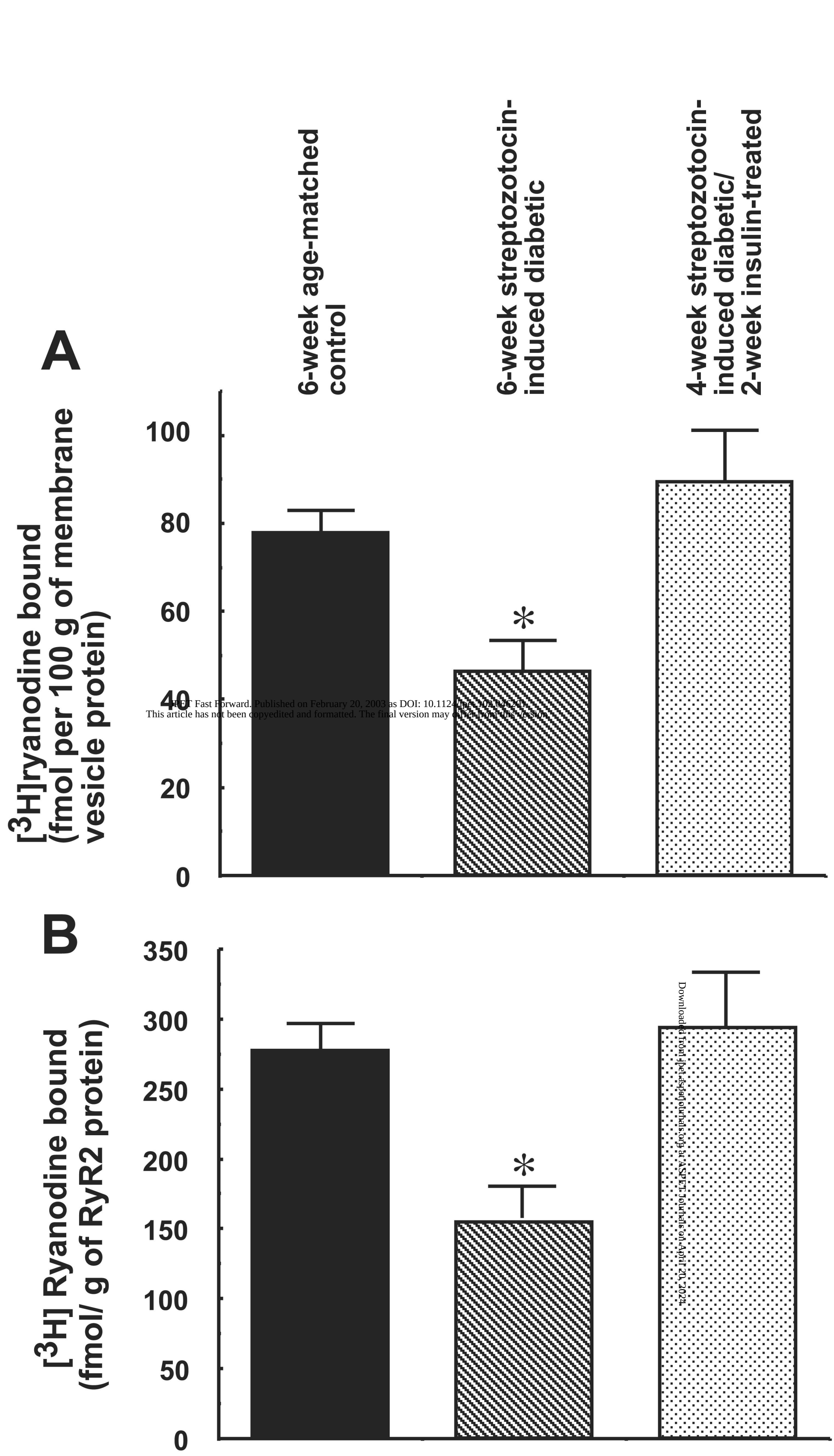

Figure 6

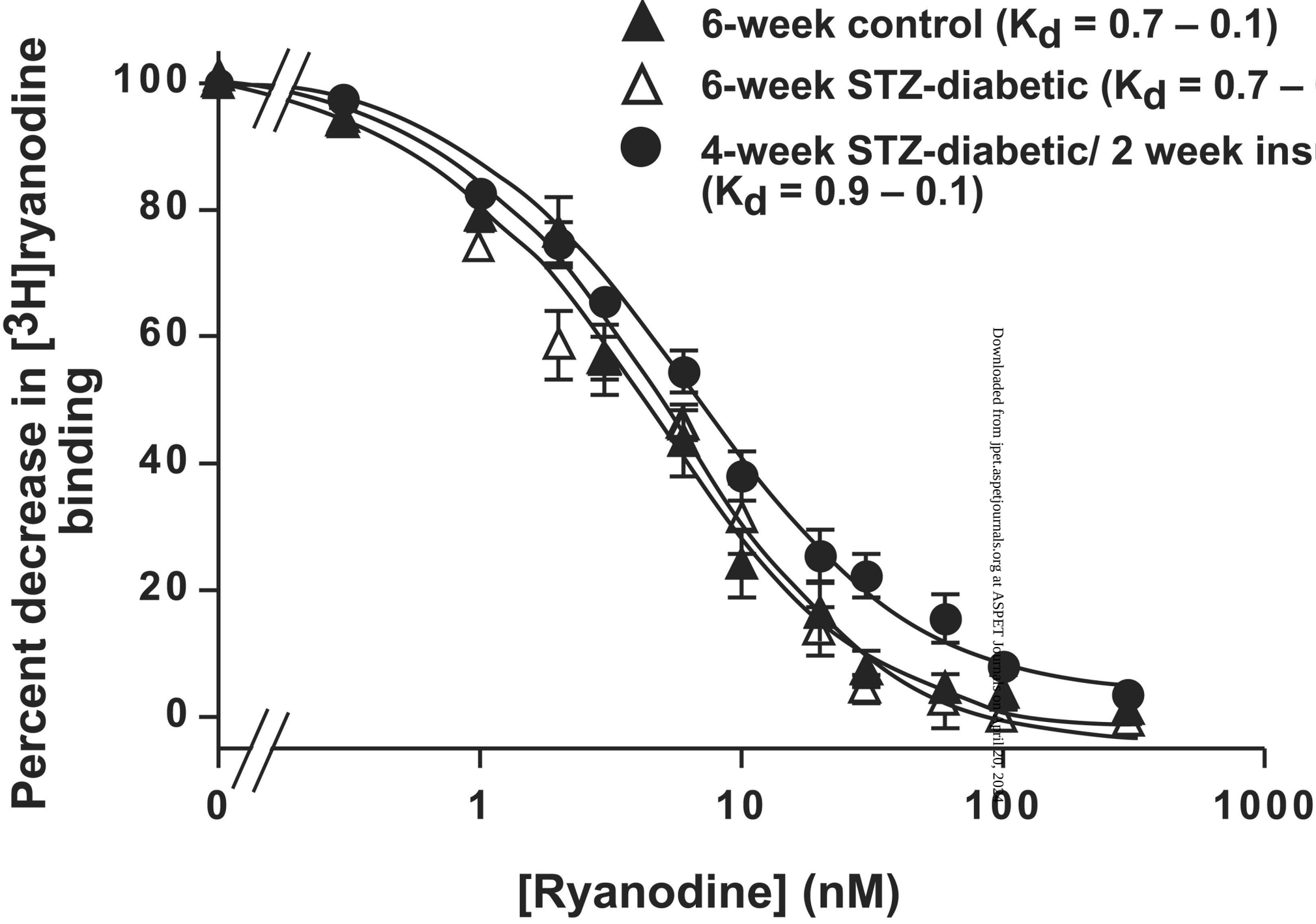

Figure 7

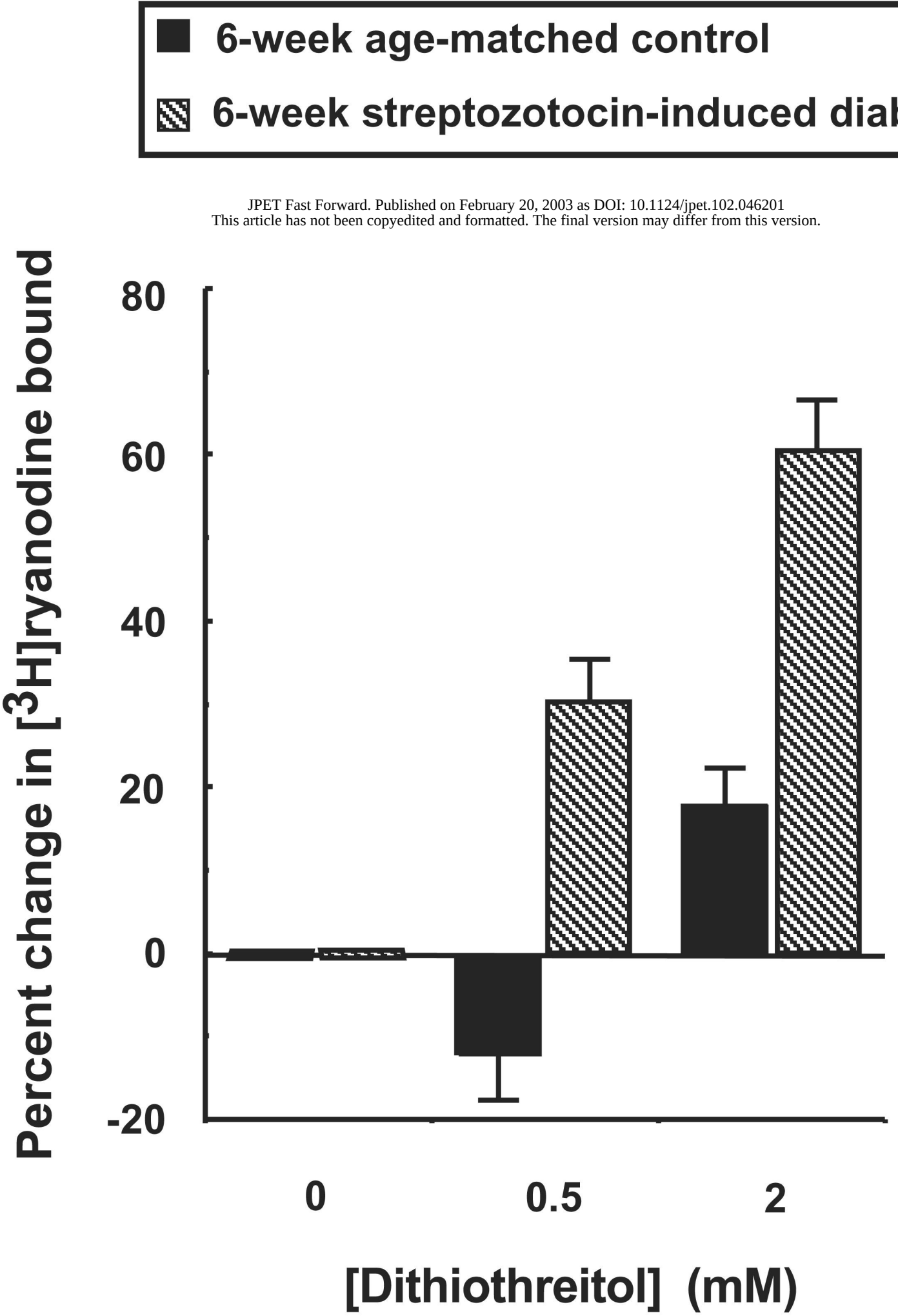

Figure 8

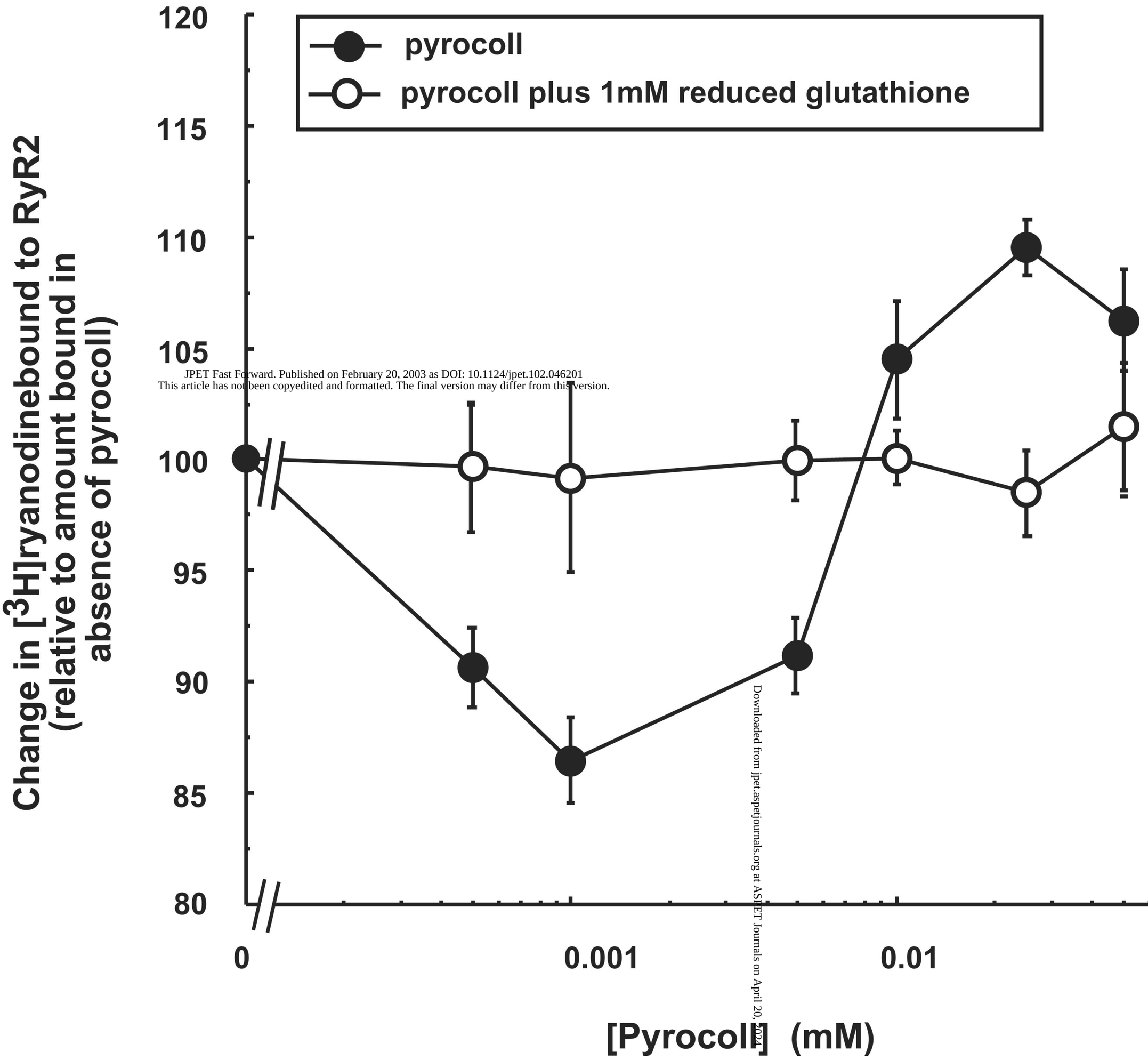

Figure 9

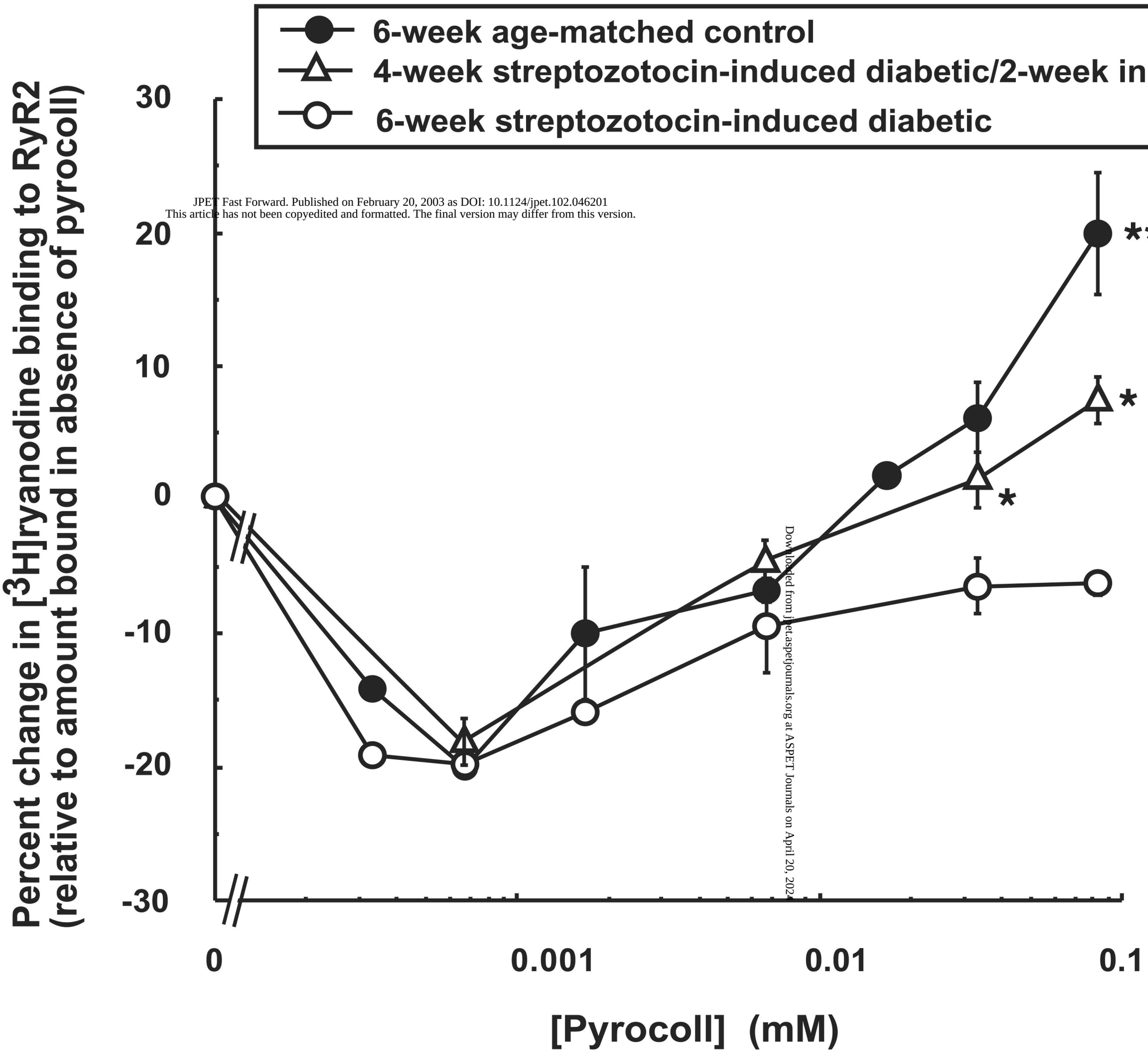

Figure 10

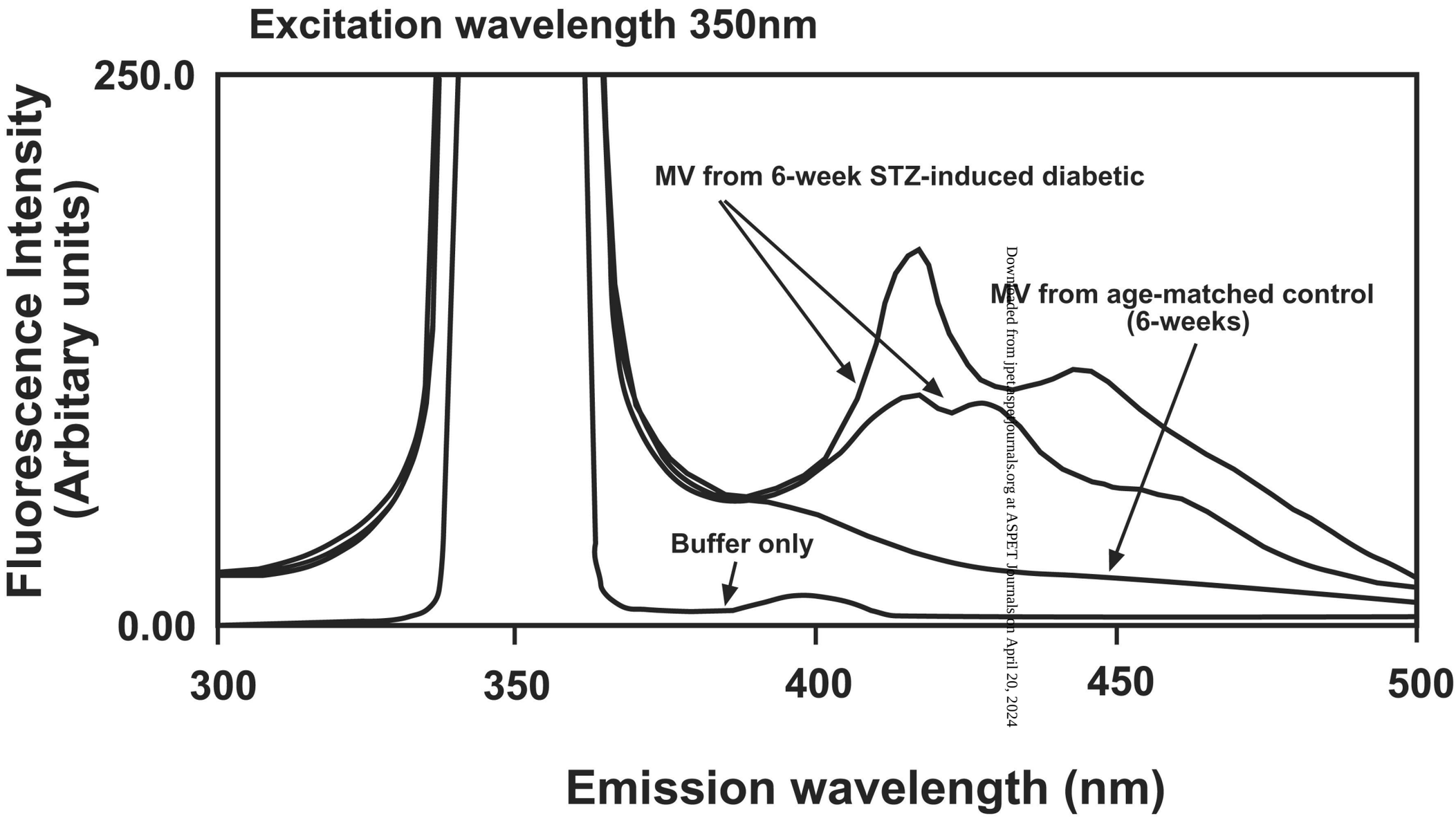

Figure 11